Electronic Supplementary Information

Unprecedented quinoid-donor-acceptor strategy to boost carrier mobilities of semiconducting polymers for organic field-effect transistors

Cheng Liu,[a] Xuncheng Liu,[,a] Guohui Zheng,[b] Xiu Gong,[b] Chen Yang,[c] Haizhen Liu,[d] Lianjie Zhang,[d] Christopher L. Anderson, [e, g], Bo He, [e, f] Lan Xie,[a] Rongzong Zheng,[a] Huanhuan Liang,[a] Quanfeng Zhou,[a] Zesheng Zhang,[d] Junwu Chen*[,d] and Yi Liu*[,e,f]*

[a] College of Materials and Metallurgy, [b] College of Physics and [c] College of Big Data and Information Engineering, Guizhou University, Guiyang 550025, China

[d] Institute of Polymer Optoelectronic Materials and Devices, State Key Laboratory of Luminescent Materials and Devices, South China University of Technology, Guangzhou 510640, China

[e] The Molecular Foundry and [f] Materials Sciences Division, Lawrence Berkeley National Laboratory, One Cyclotron Road, Berkeley, California 94720, United States

[g] Department of Chemistry, University of California, Berkeley, Berkeley, California 94720, United States

Corresponding Authors

* xcliu3@gzu.edu.cn,

* psjwchen@scut.edu.cn,

* yliu@lbl.gov.

Contents

1. General methods

Reagents were purchased from Aldrich, Acros and Energy Chemical or synthesized as described. Dry solvents were collected from a solvent purification system. Proton and carbon nuclear magnetic resonance spectra (^{1}H-NMR and ^{13}C-NMR) spectra were recorded on a JNM-ECZ400S/L1 spectrometer. All chemical shifts are quoted using the δ scale, and all coupling constants (J) are expressed in Hertz (Hz). Cyclic voltammetry (CV) was carried out on a CHI600E electrochemical workstation with platinum electrodes at a scan rate of 50 mV s^{-1} against an Ag/Ag^{+} reference electrode with nitrogen-saturated solution of 0.1 M tetrabutylammonium hexafluorophosphate (Bu_4NPF_6) in acetonitrile (CH_3CN). Potentials were referenced to the ferrocenium/ferrocene couple by using ferrocene as an internal standard. The molecular weight of polymer was determined by high temperature size exclusion chromatography (SEC) at 150 °C using a calibration curve

of polystyrene standards, with 1,2,4-trichlorobenezene as the eluent. Thermogravimetric (TGA) measurements were carried out with a NETZSCH (TG550) apparatus at a heating rate of 20 °C /min under a nitrogen atmosphere. Differential scanning calorimetry (DSC) analysis were taken on TAQ 2000 under a nitrogen atmosphere at a rate of 10 °C/min from 30 °C to 300 °C, and then cooling to 30 °C. UV-Vis-NIR spectra were recorded using a MAPADA UV-6300 spectrometer. Grazing incidence X-ray diffraction (GIXD) experiments were carried out on a Xenocs Xeuss 2.0 system with an Excillum MetalJet-D2 X-ray source operated at 70.0 kV, 2.8570 mA, and a wavelength of 1.341 Å. The grazing-incidence angle was set at 0.20°. Scattering pattern was collected with a Dectris Pilatus3R 1M area detector. Atomic force microscopy (AFM) images were obtained with a Bruker Dimension ICON, using tapping mode in air under ambient conditions.

2. Synthesis procedures

Monomer **1** was synthesized according to literature procedure.[1]

^{1}H NMR ($CDCl_3$, 400 MHz, 298K) δ = 7.04 – 6.99 (dd, *J* = 7.9, 4.6 Hz, 3H), 4.42 – 4.33 (d, *J* = 5.9 Hz, 2H), 1.99 – 1.89 (m, 1H), 1.43 – 1.22 (m, 40H), 0.89 – 0.84 (t, *J* = 6.8 Hz, 6H). ^{13}C NMR ($CDCl_3$, 101 MHz, 298K) *δ* = 157.88, 140.63, 129.88, 129.14, 128.54, 118.67, 116.45, 71.24, 37.16, 31.93, 31.62, 30.12, 29.72, 29.68, 29.37, 26.79, 22.70, 14.13.

PAQM-BT: A mixture of monomer **1** (346.84 mg, 0.306 mmol), compound **2** (118.73 mg, 0.306 mmol), $Pd_2(dba)_3$ (7 mg), tri(o-tolyl) phosphine (9 mg), three drops of N-methyl-N,N-dioctyloctan-1-ammonium chloride (Aliquat 336), K_2CO_3 (aq. 2M, 3 mL) in toluene (10 mL) was sealed in a Ar_2 flushed vessel and heated to 90 °C while stirring for 3 days. After cooling down, the mixture was precipitated into methanol. The precipitate collected

from filtration was subjected to Soxhlet extraction with methanol, acetone, ethyl acetate and $CHCl_3$ successively. The $CHCl_3$ fraction was concentrated and precipitated into methanol. The polymer (87%) was collected by filtration. M_n=16196, M_w=40813, PDI =2.5.

3. Fabrication and characterization of field effect transistors (OFETs)

Polymer thin film field effect transistors were fabricated in a typical bottom-gate, top-contact architecture. Transistors were fabricated with heavily n-doped Si as the gate electrode, Au as both source and drain electrodes. Substrates were cleaned by successive sonication with soap water, deionized water, acetone and ethanol. Then the substrate gate dielectric layers were modified by *n*-octadecyltrichlorosilane (OTS) by submersion in a solution of OTS in toluene. Solutions of polymers in DCB/CF (1:6 volume ratio, 5mg/ml) were spin-coated (3000 rpm, 30 s) onto the OTS treated substrates to form polymer thin films. When thermal treatment was noted, the polymer films were annealed at 150 °C or 250 °C for 10 minutes on a hotplate in a nitrogen glovebox. Gold contacts (40 nm) were evaporated on the polymer film layer through a metal mask to define channels of 150 μm in length and 967 μm in width. The film thickness of the devices ranges from 60 to 100 nm. Field effect mobility was calculated from the standard equation for saturation region in metal-dioxide-semiconductor field effect transistors: $I_{ds} = \mu (W/2L) C_i (V_g - V_t)^2$, where I_{ds} is drain-source current, μ is field effect mobility, W and L are the channel width and length, C_i is the capacitance per unit area of the gate insulator (C_i = 10 nF/cm^2), V_g is the gate voltage and V_t is the threshold voltage.

4. Theoretical calculations

For simplicity, the alkyl chains at the oxygen atoms were all replaced by methyl groups. Density functional theory (DFT) calculations of a dimer segment of each of the three polymers were performed using Gaussian 09[2] at the B3LYP[3]/6-311g (d, p)[4, 5] level with the D3 (BJ) empirical dispersion correction.[6] The calculation of band structures and density of states of the polymers were performed using Vienna *ab initio* simulation package (VASP)[7] with the Perdew-Burke-Ernzerhof (PBE) functional instead of B3LYP functional due to its mild demands of computational resources and the importance of being consistent with previous related studies.[8] Uniform 21 × 1 × 1 Monkhorst-Pack *k*-point mesh was used for structural optimization. The energy cut off for the plane-wave expansion was set to 400 eV and the force criteria was less than 0.05eV/Å. 41 *k*-points were calculated between the gamma point and the edge of the first BZ to afford band structure and density of states. The hole effective mass (m_h*)[9] for 1D crystal is calculated based on band structure by with the equation:

$m_h^* = h^2 / (d^2E/dk^2)$

Where E is the band energy and *k* is the electron wave vector along backbone direction.

5. Additional graphs

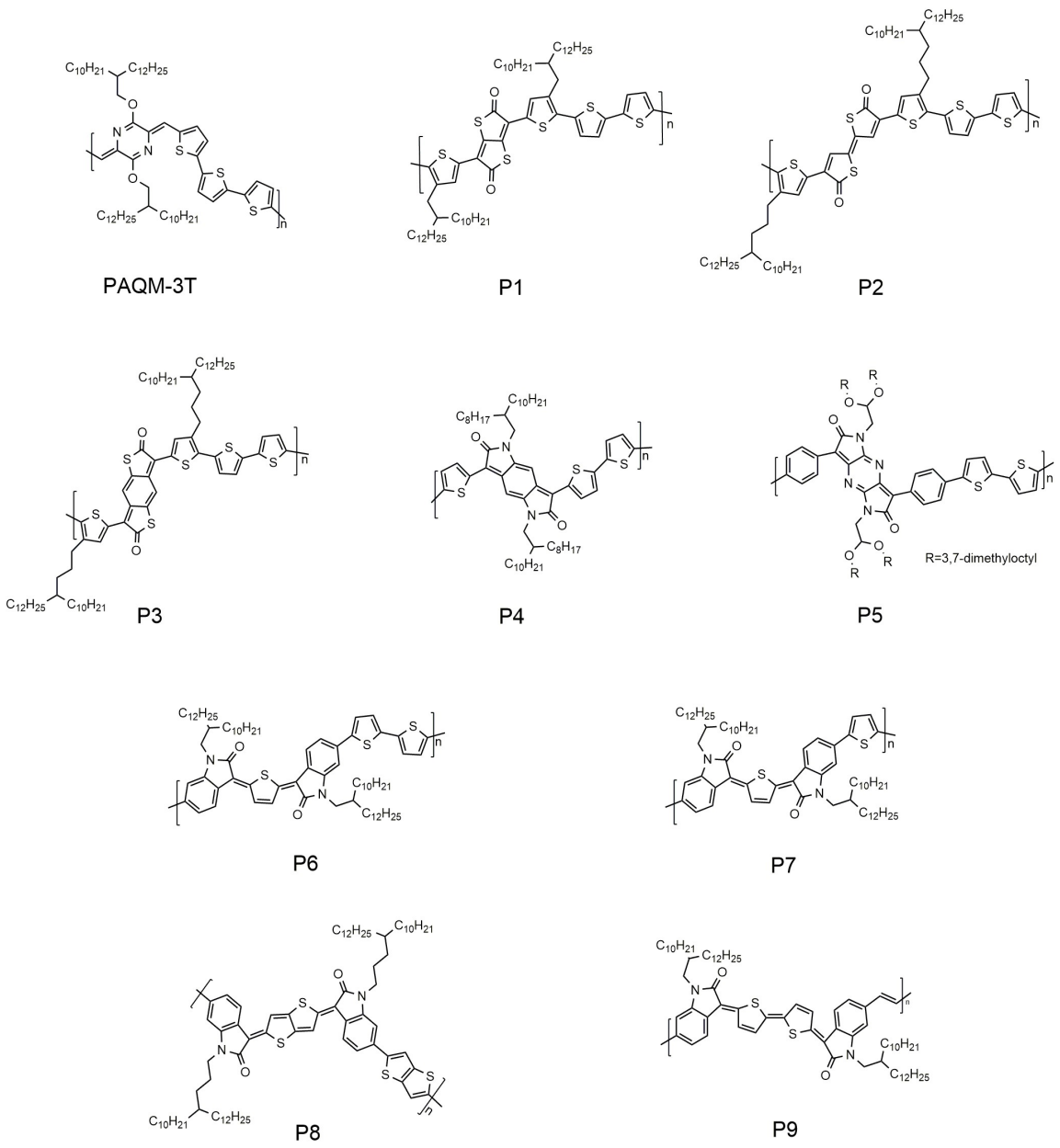

Figure S1. Chemical structures from the literature of typical quinoidal-aromatic polymers based on ground-state quinoidal units.

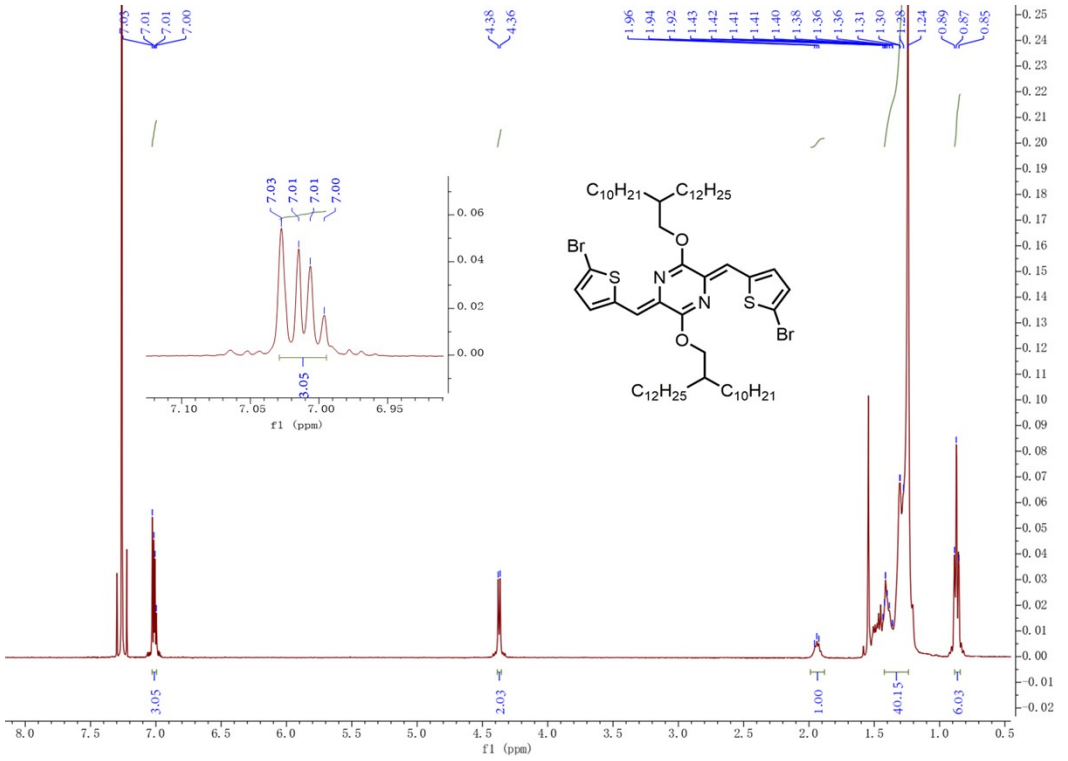

Figure S2. [1]H NMR spectrum of monomer **1** (CDCl3, 298 K).

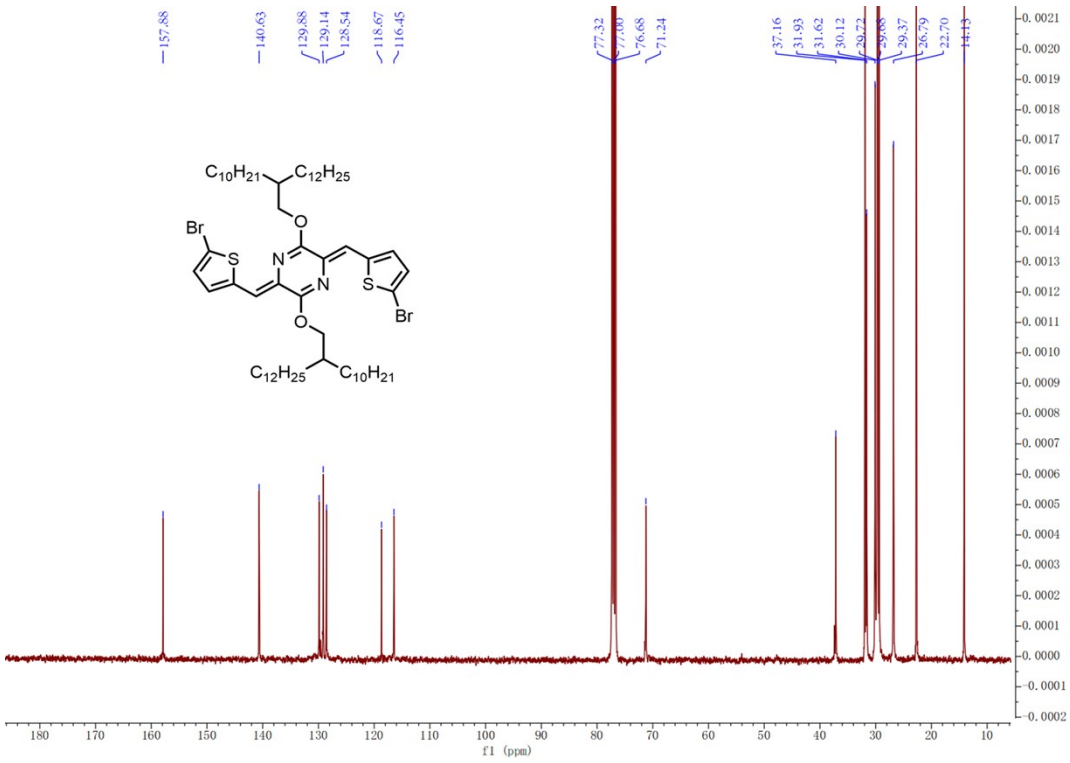

Figure S3. [13]C NMR spectrum of monomer **1** ($CDCl_3$, 298 K).

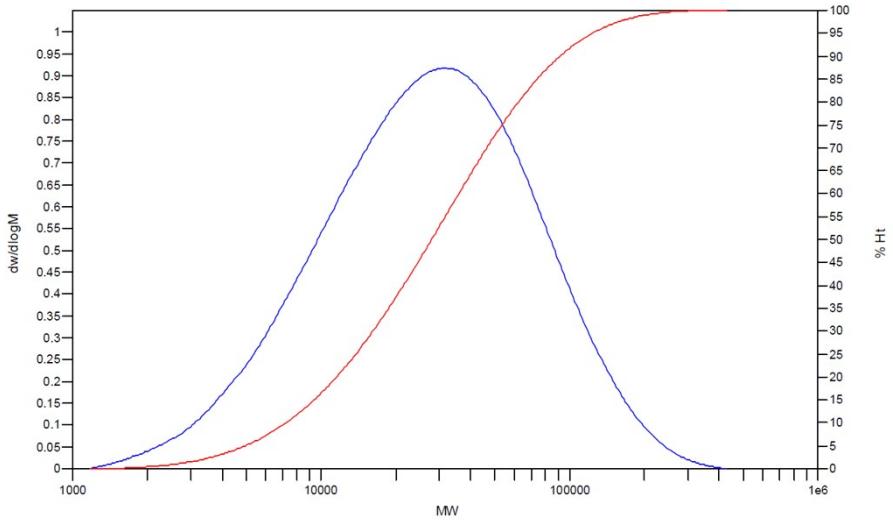

Figure S4. SEC distribution plots of PAQM-BT with 1,2,4-trichlorobenezene as the eluent at 150 °C.

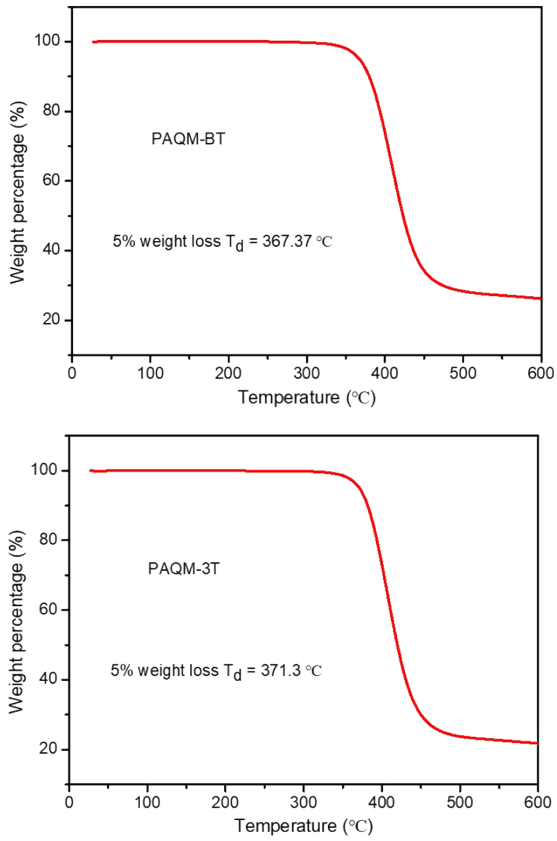

Figure S5. Thermogravimetric analysis (TGA) for PAQM-BT and PAQM-3T.

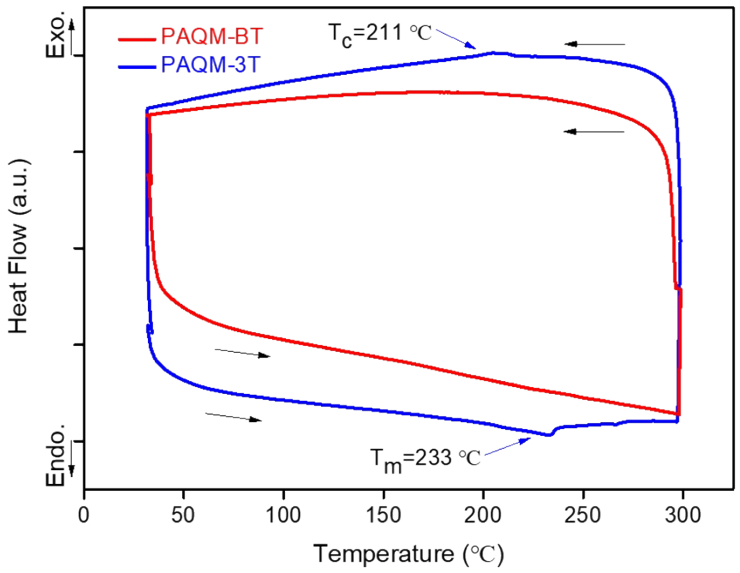

Figure S6. Differential scanning calorimetry (DSC) analysis curves of PAQM-BT and PAQM-3T.

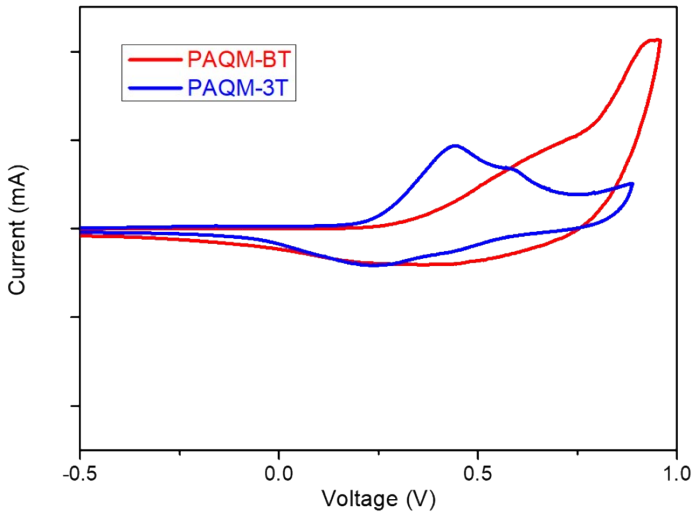

Figure S7. Cyclic voltammetry curves of PAQM-BT and PAQM-3T at scan rate of 100 mV/s. The potential is referenced to Fc/Fc^+.

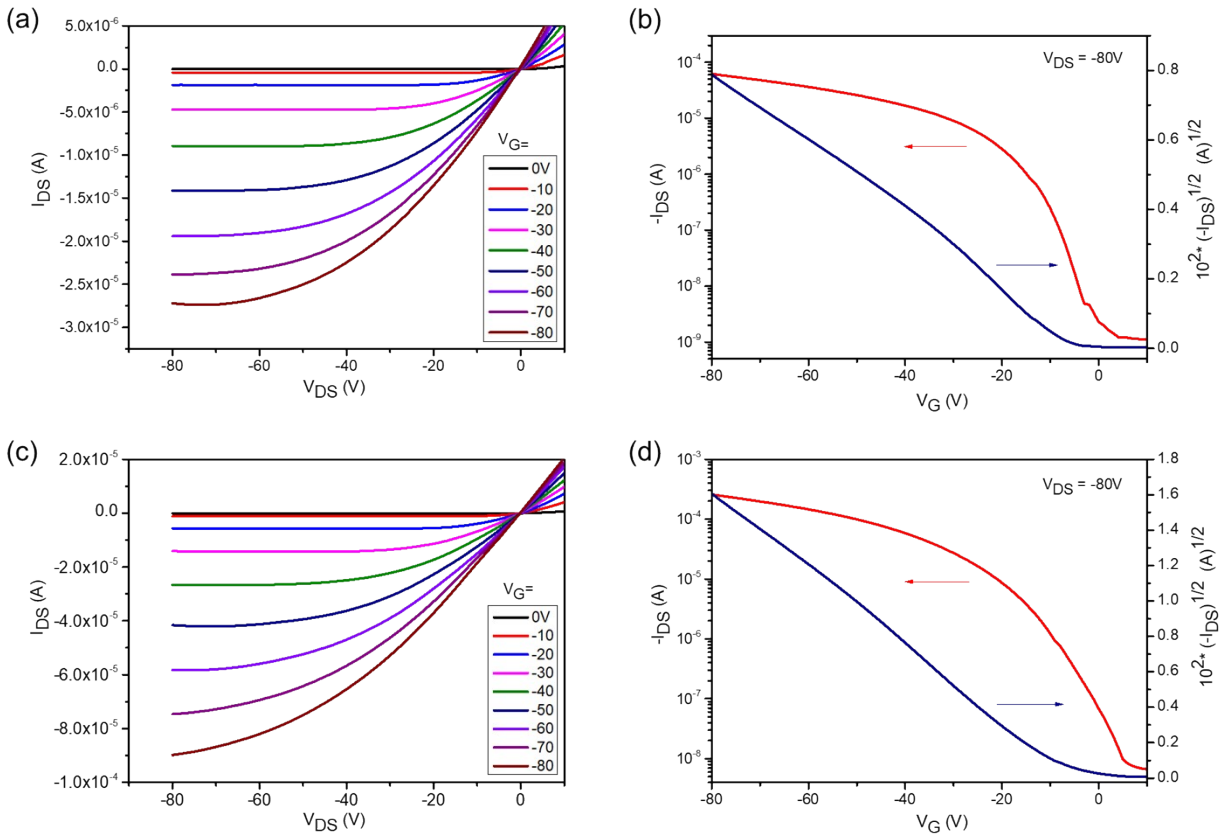

Figure S8. Output (a and c) and transfer curves (b and d) of PAQM-BT OFET devices based on as-cast film (a and b) and 150 °C annealed film (c and d).

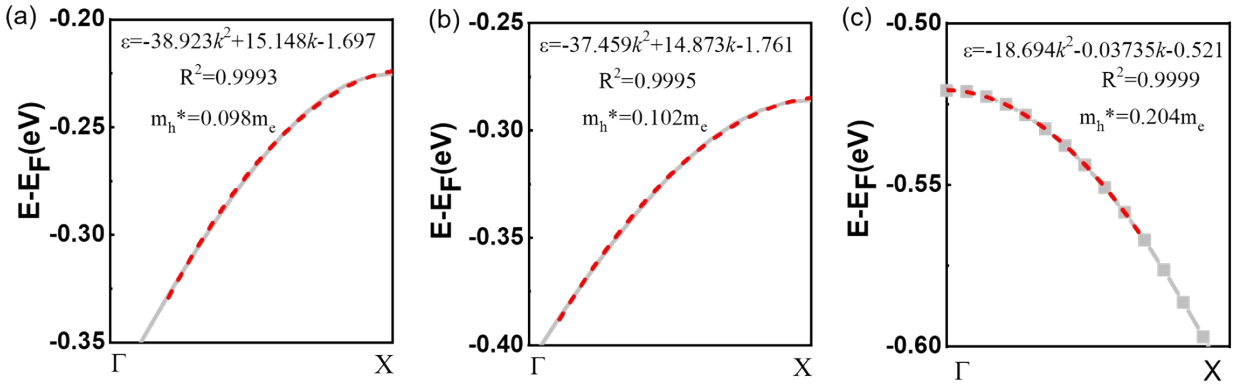

Figure S9. Curve fitting based on band structure to obtain the hole effective mass for (a) PAQM-BT, (b) PAQM-3T and (c) PT3B1.

6. Complementary data

Table S1. Summary of OFET device data for typical quinoidal-aromatic polymers characterized by conventional spin-coating deposition methods.

Polymer	HOMO/LUMO (eV)	μ_h[a] ($cm^2V^{-1}s^{-1}$)	I_{on}/I_{off}	Device structure	Literature
PAQM-BT	**–5.14/–3.84**	**5.10/4.35**	**10^3-10^4**	**BGTC (air)**	**This work**
PAQM-3T	–5.02/–3.53	0.54/0.47	10^4-10^5	BGTC (vacuum)	*J. Am. Chem. Soc*. 139, **2017**, 8355.
P1	–5.30/–4.10	1.38/0.66	10^8	BGTC (air)	*J. Mater. Chem. C* **2014**, 2, 2307.
P2	–5.20/–3.77	-/0.16	10^2	BGTC (air)	*J. Am. Chem. Soc*. 138, **2016**, 7725.
P3	–5.02/–4.04	-/0.3	10^2	BGTC (air)	*J. Am. Chem. Soc*. 138, **2016**, 7725.
P4	–5.27/–4.24	0.2/-	10^5	TGBC (N_2)	*Chem. Commun*. 49, **2013**, 4465.
P5	–5.59/–4.31	6.6×10^{-2}/-	10^5-10^6	BGBC (air)	*Chem. Commun*. 49, **2013**, 484.
P6	–5.11/–3.55	2.77/1.33[b]	10^6	TGBC (N_2)	*Adv. Mater*. **2018**, 30, 1706557.
P7	–5.24/–3.56	3.6/1.37	10^5-10^6	TGBC (N_2)	*Adv. Mater*. **2018**, 30, 1706557.
P8	–5.19/–3.36	0.13/-	10^4-10^5	BGTC (vacuum)	*Macromolecules* **2019**, 52, 4749.
P9	–5.08/–3.79	0.52/0.25	10^3	TGBC (N_2)	*Polym. Chem.* **2017**, 8, 361.

[a] Mobilities were provided in the "highest/average" form. [b] value could be up to "8.09/5.25" using an optimized and non-conventional off-center spin-coating deposition method.

7. References.

1. X. Liu, B. He, C. L. Anderson, J. Kang, T. Chen, J. Chen, S. Feng, L. Zhang, M. A. Kolaczkowski, S. J. Teat, M. A. Brady, C. Zhu, L.-W. Wang, J. Chen and Y. Liu, *J. Am. Chem. Soc.*, 2017, **139**, 8355-8363.
2. Gaussian 09, Revision E.01, Frisch, M. J., Trucks, G. W., Schlegel, H. B., Scuseria, G. E., Robb, M. A., Cheeseman, J. R., Scalmani, G., Barone, V., Mennucci, B., Petersson, G. A., Nakatsuji, H., Caricato, M., Li, X., Hratchian, H. P., Izmaylov, A. F., Bloino, J., Zheng, G., Sonnenberg, J. L., Hada, M., Ehara, M., Toyota, K., Fukuda, R., Hasegawa, J., Ishida, M., Nakajima, T., Honda, Y., Kitao, O., Nakai, H., Vreven, T., Montgomery, J. A., Jr., Peralta, J. E., Ogliaro, F., Bearpark, M.,

Heyd, J. J., Brothers, E., Kudin, K. N., Staroverov, V. N., Kobayashi, R., Normand, J., Raghavachari, K., Rendell, A., Burant, J. C., Iyengar, S. S., Tomasi, J., Cossi, M., Rega, N., Millam, J. M., Klene, M., Knox, J. E., Cross, J. B., Bakken, V., Adamo, C., Jaramillo, J., Gomperts, R., Stratmann, R. E., Yazyev, O., Austin, A. J., Cammi, R., Pomelli, C., Ochterski, J. W., Martin, R. L., Morokuma, K., Zakrzewski, V. G., Voth, G. A., Salvador, P., Dannenberg, J. J., Dapprich, S., Daniels, A. D., Farkas, Ö., Foresman, J. B., Ortiz, J. V., Cioslowski, J., Fox, D. J. Gaussian, Inc., Wallingford CT, 2009.

3. A. D. Becke, *J. Chem. Phys.*, 1993, **98**, 5648-5652.
4. W. J. Hehre, R. Ditchfield and J. A. Pople, *J. Chem. Phys.*, 1972, **56**, 2257-2261.
5. P. C. Hariharan and J. A. Pople, *Theor. Chim. Acta*, 1973, **28**, 213-222.
6. S. Grimme, S. Ehrlich and L. Goerigk, *J. Comput. Chem.*, 2011, **32**, 1456-1465.
7. G. Kresse and J. Furthmüller, *Phys. Rev. B*, 1996, **54**, 11169-11186.
8. P. E. Blöchl, *Phys. Rev. B*, 1994, **50**, 17953-17979.
9. B. B.-Y. Hsu, C.-M. Cheng, C. Luo, S. N. Patel, C. Zhong, H. Sun, J. Sherman, B. H. Lee, L. Ying, M. Wang, G. Bazan, M. Chabinyc, J.-L. Brédas and A. Heeger, *Adv. Mater.*, 2015, **27**, 7759-7765.